Advances in Science and Technology Research Journal

Advances in Science and Technology Research Journal, 2026, 20(10), 32–38
https://doi.org/10.12913/22998624/224291
ISSN 2299-8624, License CC-BY 4.0

Received: 2026.06.01
Accepted: 2026.08.13
Published: 2026.09.01

Performance characteristics of a high-density hybrid rocket fuel with nitrous oxide

Bartosz Dąbrowski[1], Katarzyna Ignatowicz[2*]

[1] Faculty of Power and Aeronautical Engineering, Warsaw University of Technology, ul. Nowowiejska 24, 00-665 Warsaw, Poland
[2] Faculty of Civil Engineering and Environmental Sciences, Bialystok University of Technology, ul. Wiejska 45a, 15-351 Białystok, Poland
* Corresponding author's e-mail: k.ignatowicz@pb.edu.pl

ABSTRACT

This study presented experimental characterization of the HyPEx-B high-density hybrid rocket fuel comprising aluminum, bismuth trioxide, and hydroxyl-terminated polybutadiene (HTPB) binder with nitrous oxide across a range of oxidizer-to-fuel ratios near the theoretical performance optimum. The oxidizer-to-fuel ratio was varied by changing grain length while all other motor hardware remained identical to the previous study. Fuel regression was quantified by comparing grain mass on a calibrated scale and by volumetric analysis of longitudinal cross-sections, with both methods showing good agreement. Peak delivered specific impulse of 200.8 s was measured at O/F=2.98 with a combustion efficiency of 97% compared to AFAL and peak volumetric specific impulse of 1818 Ns/dm^3 at O/F=2.62. While mass-specific impulse is comparable to reference HTPB-based formulations, the volumetric specific impulse shows a consistent advantage attributable to the high-density bismuth trioxide loading. The paper also briefly explored potential paths for the future development of this type of composition.

Keywords: nitrous oxide, volumetric specific impulse, hybrid rocket motor, oxidizer to fuel ratio, bismuth trioxide, hydroxyl-terminated polybutadiene.

INTRODUCTION

Hybrid rocket propulsion offers a compelling combination of safety, simplicity, and moderate cost for small launch and experimental rocketry applications [1, 2]. Nitrous oxide is the preferred oxidizer at small scales due to its self-pressurizing behavior and ease of handling [3], but the conventional and widely used hydroxyl-terminated polybutadiene (HTPB) fuel exhibits limited volumetric specific impulse, which is a key figure of merit for volume constrained vehicles [4]. Adding energetic metal powders to HTPB increases both heat of combustion and fuel density, with prior work by Scaramuzzino et al. [5] demonstrating improved regression rate and calculated specific impulse for aluminum-doped HTPB/N_2O systems.

The predecessor to this work [6] developed and computationally evaluated two formulations under the acronym HyPEx (Hybrid Propellant Experiment): HyPEx-A (HTPB, Al, parlon) and HyPEx-B, which extends HyPEx-A with bismuth trioxide. The Bi_2O_3 acts as a condensed phase oxidizer through thermite-type reactions with aluminum at the fuel surface [7] and substantially increases fuel density. A single hot fire of HyPEx-A confirmed potential performance gains while HyPEx-B was not tested. This paper bridges that gap. Four static fire tests of HyPEx-B are reported, covering O/F = 2.2 – 4.1 by varying the grain length. Delivered specific and volumetric specific impulses are compared against AFAL predictions and the references above.

STUDY METHODOLOGY

Propellant formulation

The HyPEx-B formulation used in this study was adjusted from the composition reported in the predecessor work [6], which specified constituent proportions in volumetric fractions. Those fractions with HyPEx-B resulted in a metallic powder loading that rendered the formulation impossible to cast reliably. Aluminum and bismuth trioxide contents were therefore reduced on a mass fraction basis to achieve a pourable consistency with solids loading of 60% while preserving the volumetric energy density intent. The as-cast composition and measured composition density are given in Table 1.

Thermochemical simulations

Thermochemical performance predictions were obtained using the AFAL Specific Impulse Program [8], an equilibrium thermochemical code that computes adiabatic flame temperature, characteristic exhaust velocity, and frozen-flow specific impulse for user-defined propellant compositions at specified chamber pressure and nozzle expansion ratio. Pre-test motor simulations were carried out using the Hybrid Rocket Analysis Program [9], based on the blowdown tank model of Newlands [10], to select grain lengths and verify that web thickness at burnout was sufficient. Initial regression rate estimates were density-scaled from the HTPB/N_2O correlation of Doran et al. [11]. Calculations were performed across O/F = 0.75–6.5 at nine chamber pressures spanning the expected operating range to generate theoretical *Isp* (specific impulse, m/s or Ns/kg) and Isp_{vol} (volumetric specific impulse, Ns/dm^3 J_{total} total impulse, Ns) curves. The frozen-product assumption at the nozzle throat was applied throughout the study. This is conservative relative to shifting equilibrium and gives a lower bound on theoretical *Isp*. Propellant system density (ρ_{prop}) was computed from the mixture rule

$$\rho_{prop} = \frac{1+\xi}{\frac{1}{\rho_f} + \frac{\xi}{\rho_{ox}}} \tag{1}$$

where: ρ_f = 1607 kg/m^3 for the fuel and the temperature-dependent liquid N_2O density from Ferreira and Lobo [12].

For all propellant density and Isp_{vol} calculations in this paper, ρ_{ox} = 800 kg/m^3 was used, corresponding to saturated liquid N_2O at approximately 18 °C. Test-day oxidizer tank temperatures ranged from 16.5 to 18.4 °C, giving ρ_{ox} within 1% of this reference value across all tests.

Table 1. HyPEx-B fuel composition and cast density

Ingredient	Mass fraction	Density (g/cm^3)
Aluminum powder	30.0%	2.70
Bi_2O_3	24.0%	8.90
Parlon	6.0%	1.50
HTPB binder	39.9%	0.90
Other additives	0.1%	—
Cast density		1607 kg/m^3

Motor configuration and test campaign

All four tests used the same motor hardware as the predecessor HyPEx-A study (Table 2). Grains were cast with fixed outer and initial port diameters; only grain length was varied between tests to shift the average O/F. A longer grain provides a larger burning surface relative to the fixed oxidizer supply, driving the operating point toward fuel-rich conditions. Initial fuel masses and corresponding grain lengths are listed in Table 3.

HyPEx-B was mixed and cast into phenolic liner tubes following the procedure of the predecessor study [6], with all test articles cast from a single batch. The oxidizer tank was filled to the target mass prior to each test and the initial tank temperature was recorded. Liquid N_2O density and saturation pressure were derived from reference correlations [3, 12]. Portions of the combustion chamber not covered by the fuel were additionally insulated using low-regression-rate phenolic to protect test hardware.

Data analysis

Specific impulse and volumetric specific impulse were derived from

$$Isp = \frac{J_{total}}{(m_{ox} + \Delta m_f)\, g_0} \tag{2}$$

$$Isp_{vol} = Isp \cdot g_0 \cdot \frac{\rho_{prop}}{1000} \tag{3}$$

Where J_{total} was obtained by numerical integration of the load cell signal, and propellant masses were determined by weighing the grain assembly and oxidizer tank before and after each firing on a calibrated scale. Fuel regression was additionally characterized by longitudinal sectioning of the recovered grains and measuring the remaining solid fraction along the grain using digital image processing methods. The mass determined by the optical method was compared with the gravimetric measurement, and both methods were found to be in generally good agreement with minor differences experienced at higher O/F ratios due to a larger presence of phenolic insulators. Average regression rate was computed as $\dot{r} = (\bar{D}_f - D_i)/(2t_b)$ ($\dot{r}$ – average fuel regression rate, mm/s) with burn time extracted from the thrust curve, but due to oxidizer flow rate being fairly constant across the tests, it was not deemed useful for this study. Combustion efficiency was estimated as $\eta_{Isp} = Isp_{del}/Isp_{th}$, with the theoretical value interpolated from AFAL at the measured average O/F = ξ and nominal chamber pressure (η_{Isp} – combustion efficiency, ξ – oxidizer-to-fuel mass ratio; used interchangeably with O/F).

Measurement uncertainty

The load cell contributes negligibly to *Isp* uncertainty, with a rated accuracy of ±0.002% of full scale. The dominant source is the gravimetric determination of burnt fuel mass. Two pre/post weighings each carry a balance resolution of ±0.5 g, giving a combined standard uncertainty of 0.71 g on Δm_f. Relative to consumed fuel masses of 103.8–231.3 g, this yields a fuel mass relative uncertainty of 0.31–0.68%, which propagates almost directly into *Isp*. Including the oxidizer mass and uncertainty due to phenolic liner ablation, the combined expanded uncertainty (k = 2, nominally 95% confidence) in *Isp* is ±0.8–1.5% across the four tests. These are the error bars shown in Figures 3 and 4. Uncertainty in Isp_{vol} additionally includes the variation in ρ_{ox} from the test day temperature range. Because the AFAL theoretical baseline is interpolated at the measured O/F, and O/F carries the same gravimetric uncertainties, combustion efficiency values should be interpreted with the caveat that a systematic error in the consumed-mass ratio of the magnitude noted would shift the reported efficiency by up to 1–2 percentage points.

Each O/F condition was tested only once, which constitutes a significant limitation of the present campaign. No repeatability assessment is therefore possible, and confidence intervals reflecting run-to-run variability cannot be reported. The trends presented in Section "Results and discussion" must be treated as indicative only and should not be interpreted as statistically confirmed relationships. The campaign is intended as a first characterization of the HyPEx-B delivered performance to guide formulation and grain geometry choices for future work involving repeated tests at each operating point, at larger scales more representative of a flight vehicle.

Table 2. Fixed motor parameters [6]

Parameter	Value	Unit
Oxidizer tank volume	800	cm^3
Grain outer diameter	38	mm
Initial port diameter	20	mm
Initial web thickness	9	mm
Injector diameter	3.3	mm
Injector C_d	0.56	—
Nozzle throat diameter	8	mm

Table 3. Test matrix, numbered by firing order

Test	Grain length (mm)	Initial fuel mass (g)	Target O/F
T1	228	300	2
T2	122	160	4
T3	152	200	3
T4	190	250	2.5

RESULTS AND DISCUSSION

Thermochemical predictions

AFAL simulations predict peak specific impulse for HyPEx-B/N_2O near O/F≈2.5, with the optimum shifting slightly with chamber pressure. This lies far below the O/F=6–8 range typical of pure HTPB because Bi_2O_3 provides internal oxygen through condensed-phase thermite reactions with aluminum [7], reducing the stoichiometric demand for external N_2O. Theoretical *Isp* and Isp_{vol} curves are presented alongside the experimental results and reference data in Figures 3 and 4.

Static fire tests

All four tests proceeded without anomalies. Overlaid thrust curves are shown in Figure 1. A combined test conditions and performance table is given in Table 4. Post-fire inspection of the recovered grains revealed that, compared to aluminum-only HTPB formulations, the addition of bismuth trioxide produced a noticeably shinier, more metallic-looking regression surface and a marked increase in slag buildup on the nozzle inlet and aft-chamber walls, consistent with the higher density and lower volatility of bismuth combustion products.

Specific impulse and combustion efficiency

Specific impulse rises from 186.7s at O/F=2.20 to a broad plateau of 197–201 s across O/F=2.6–4.1. Each operating point was tested once, and the trends discussed below are therefore indicative rather than statistically confirmed, and repeatability tests at each O/F would be required to establish significance. Test T1 exhibited noticeable flame instabilities, visible as periodic thrust oscillations in the trace and captured in four sequential frames in Figure 2. The thrust RMS noise quantifies this clearly: T1 recorded 8.39 N compared to 2.58, 2.24, and 1.97 N for T2, T3, and T4, respectively, a factor of 3–4 higher than the stable tests. Combustion efficiency was correspondingly the lowest of the campaign at 88.6%. Tests T2, T3, and T4 showed stable combustion throughout, with efficiencies of 94.9%, 97.7%, and 98.1%, respectively, compared to AFAL predictions.

The instability in T1 is tentatively attributed to the strongly fuel-rich condition, where insufficient external N2O may limit gas-phase heat release near the fuel surface, reducing flame stabilization and potentially allowing periodic extinction and re-ignition events [13, 14]. The high metallic powder loading amplifies this effect, unburned aluminum and bismuth particles that exit the combustion zone without reacting contribute to the oscillatory behavior by intermittently releasing energy downstream, a mechanism well-documented in aluminized solid and hybrid propellants [15]. It should be noted, however, that T1 also had the longest grain of the campaign, meaning the combustion chamber acoustic length differed most from the other tests. The contribution of chamber acoustic modes or altered residence time distribution to the observed instability cannot be excluded without dedicated tests varying grain length independently of O/F.

Based on the literature, these instabilities may diminish at larger motor scales. Low-frequency instability in small-scale hybrid motors is sensitive to chamber residence time [14]. In a longer combustion chamber, aluminum and bismuth droplets would have more time to ignite and burn to completion before reaching the nozzle, potentially stabilizing the heat release distribution. Larger scale might therefore improve mean combustion efficiency and could reduce the instability observed at fuel-rich O/F in this motor, although this hypothesis requires experimental confirmation at representative scales.

A notable feature of both the Isp and Isp_{vol} data is that the experimental performance peak is shifted to higher O/F relative to the AFAL theoretical prediction. The AFAL curve peaks near O/F≈2.5, while the measured Isp and Isp_{vol} reach their maximum roughly 0.1–0.5 O/F units higher. This shift can be explained by combustion efficiency - the theoretical calculation assumes equilibrium combustion, but at fuel-rich conditions, the delivered efficiency drops sharply so the actual delivered performance peaks at a less fuel-rich operating point where efficiency is higher even

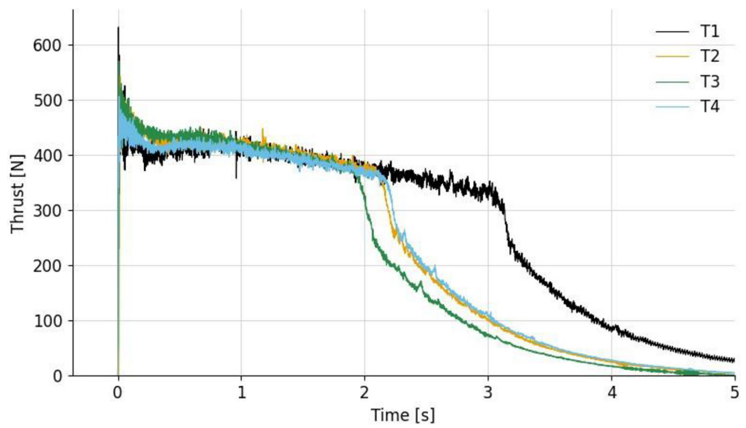

Figure 1. Overlaid thrust curves for all four tests, time-aligned to ignition

Table 4. Test conditions and derived performance

Parameter [unit]	Symbol	T1	T2	T3	T4
Grain length [mm]		228	122	152	190
Initial fuel mass [g]		300	160	200	250
Test temperature [°C]		16.5	18.4	17.9	17.3
Oxidizer mass [g]		508	424	399	406
Fuel consumed [g]		231.3	103.8	134.0	155.0
O/F [–]	ξ	2.20	4.08	2.98	2.62
Propellant density [kg/m^3]	*ρprop*	949	888	916	929
Total impulse [Ns]	*J*	1354	1022	1050	1098
Specific impulse [s]	*Isp*	186.7	197.4	200.8	199.5
Theoretical *Isp* — AFAL [s]	Isp_{th}	210.8	207.9	205.6	203.3
Combustion efficiency [–]	*ηIsp*	0.886	0.949	0.977	0.981
Vol. specific impulse [Ns/dm^3]	Isp_{vol}	1738	1719	1804	1818

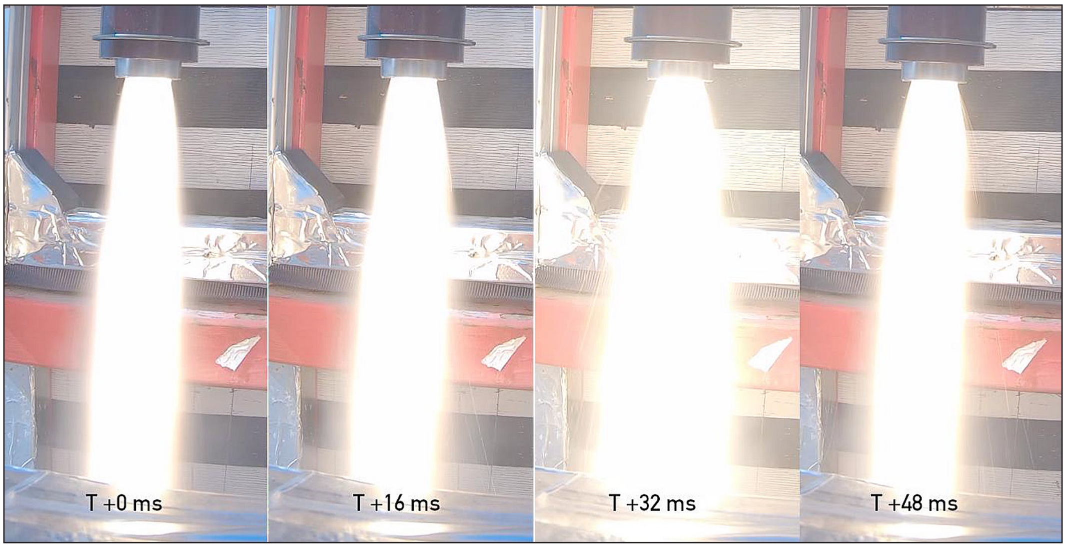

Figure 2. Four sequential frames from T1 showing flame instability events

though the theoretical ceiling is lower. In other words, the gain in combustion completeness from moving toward stoichiometric conditions outweighs the theoretical *Isp* decline, pushing the delivered optimum toward higher O/F than the equilibrium prediction suggests.

As visible in Figure 3, the delivered specific impulse of HyPEx-B is broadly competitive with, but does not clearly exceed, the reference formulations. The HTPB/N_2O data provided by Rezaei et al. [16] and the aluminium-doped HTPB results reported by Scaramuzzino et al. [5] span a comparable *Isp* range. This is physically expected: Bi_2O_3 is a heavy compound and exits partly as condensed bismuth or bismuth oxide, diluting the specific impulse relative to lighter formulations. HyPEx-B delivers no mass-specific impulse advantage and its value proposition is purely volumetric.

Volumetric specific impulse

Delivered Isp_{vol} ranges from 1719 to 1818 Ns/dm^3, with the highest value at O/F=2.62 (T4). The same rightward shift observed in *Isp* also applies here. The AFAL Isp_{vol} curve peaks near O/F≈2.0–2.5, but the experimental maximum lies at O/F=2.62, again reflecting the efficiency penalty at very fuel-rich conditions that suppresses the delivered performance below the theoretical envelope. HyPEx-B sits consistently above both reference datasets: the gain over Rezaei et al. [16] reaches 7–15% at comparable O/F, and the gain over Scaramuzzino et al. [5] is 5–8%. This

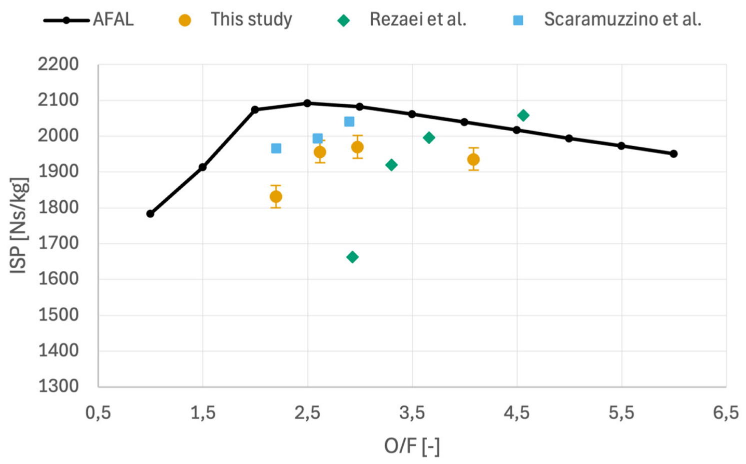

Figure 3. Delivered specific impulse vs O/F: AFAL prediction, this study, Rezaei et al. HTPB [16], derived Scaramuzzino et al. HTPB doped with Al [5]

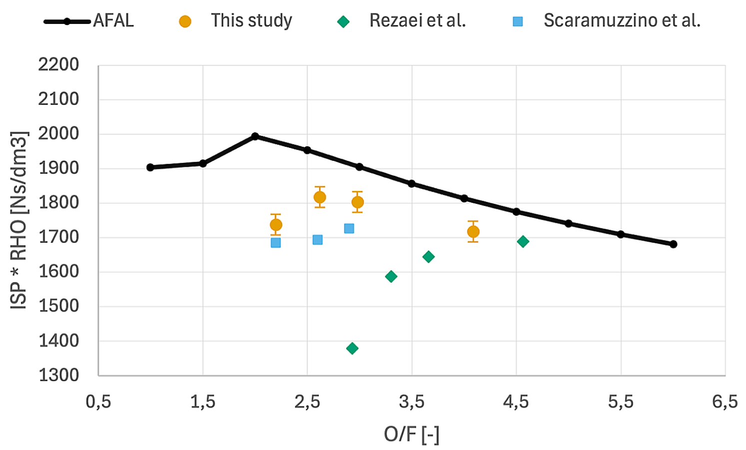

Figure 4. Delivered volumetric specific impulse vs O/F: AFAL prediction, this study, Rezaei et al. [16], Scaramuzzino et al. [5]

advantage originates directly from the higher fuel density, which increases ρ_{prop}, and results in more total impulse at the same O/F (Figure 4).

CONCLUSIONS

Four static fire tests of HyPEx-B with nitrous oxide have been conducted across O/F=2.2–4.1. Peak delivered specific impulse of 200.8 s was measured at O/F=2.98, approximately 0.5 units higher than the AFAL equilibrium optimum. This rightward shift is attributed to the sharp fall in combustion efficiency under fuel-rich conditions, which depresses delivered performance below the theoretical ceiling and pushes the effective optimum toward higher O/F. This is a consistent and physically explainable result. Mass-specific impulse is comparable to reference HTPB and aluminized-HTPB formulations but does not exceed them, reflecting the mass penalty of the heavy Bi_2O_3 component. Delivered Isp_{vol} of 1719–1818 Ns/dm^3 consistently exceeds both the pure HTPB and the Al-HTPB calculated by 5–15%, confirming the volumetric performance advantage of the high-density formulation.

HyPEx-B is a promising formulation for volume-constrained hybrid propulsion, but Bi_2O_3 is an expensive specialty compound that limits batch size and repeated testing. Future development should evaluate replacement with denser metal oxides that are already used in aerospace propulsion and available at lower cost such as copper or iron compounds. Such oxides could replicate or improve the propellant density while reducing material cost and potentially offering better characterized nozzle deposit behavior.

Acknowledgements

The authors wish to thank the Baltic Space NGO (https://balticspace.eu) and Stanisław Mazela from Universitat Politècnica de València for supporting and facilitating this research.

The research was carried out as part of research work no. WZ/WB–IIŚ/2/2024 at the Bialystok University of Technology and financed from a subsidy provided by the Ministry of Education and Science.

REFERENCES

1. Jackson A. The nitrous oxide hybrid rocket motor. In: Journal of Pyrotechnics (1997). Originally published in High Power Rocketry, May 1995; 20.
2. Okniński A., et al. Hybrid rocket propulsion technology for space transportation revisited – propellant solutions and challenges. FirePhysChem (2021). https://doi.org/10.1016/j.fpc.2021.11.015
3. Whitmore S.A. and Chandler S.N. Engineering model for self-pressurizing saturated N_2O-propellant feed systems. In: Journal of Propulsion and Power, 2010.
4. Whitmore S., Peterson Z., and Eilers S. Analytical and experimental comparisons of HTPB and ABS as hybrid rocket fuels. In: 47th AIAA/ASME/SAE/ASEE Joint Propulsion Conference & Exhibit. https://doi.org/10.2514/6.2011-5909
5. Scaramuzzino F. et al. Paraffin-based and metal-loaded HTPB fuel regression-rates study in a lab-scale hybrid rocket fed with N_2O. In: 5th European Conference for Aeronautics and Space Sciences (EUCASS). 2013.
6. Dąbrowski B. and Ignatowicz K. Methods of increasing volumetric specific impulse in HTPB based hybrid rocket motors. Advances in Science and Technology Research Journal, 2025, 19(10):15-24. https://doi.org/10.12913/22998624/207553
7. Piekiel N.W. et al. Initiation and reaction in Al/Bi_2O_3 nanothermites: Evidence for the predominance of condensed phase chemistry. Combustion Science and Technology, 2014.
8. Selph C.C. and Hall R. AFAL Specific Impulse Program. In: Phillips Lab., Propulsion Directorate, RKCC, Edwards AFB, CA, code updated periodically, 1992.
9. Nickel R. Hybrid Rocket Analysis Program. 2023. https://github.com/rnickel1/HRAP_Source
10. Newlands R.M. The science and design of the hybrid rocket engine. 2017.
11. Eric Doran et al. Nitrous oxide hybrid rocket motor fuel regression rate characterization. In: 43rd AIAA/ASME/SAE/ASEE Joint Propulsion Conference & Exhibit, 2007. https://doi.org/10.2514/6.2007-5352
12. Ferreira A.G.M. and Lobo L.Q. Nitrous oxide: Saturation properties and the phase diagram. Journal of Chemical Thermodynamics, 2009. https://doi.org/10.1016/j.jct.2009.06.017
13. Kim S. et al. Equivalence ratio variation and combustion instability in hybrid rocket. Journal of Mechanical Science and Technology 2019; 33(10): 5005–5013. https://doi.org/10.1007/s12206-0190942-5
14. De Luca L.T. et al. Low frequency instability in laboratory-scale hybrid rocket motors. Aerospace Science and Technology, 2015. https://doi.org/10.1016/j.ast.2015.01.016
15. Gallier S. and Godfroy F. Aluminum combustion driven instabilities in solid rocket motors. Journal of Propulsion and Power, 2009; 25(2): 509–521. https://doi.org/10.2514/1.37664
16. Rezaei H., Soltani M.R., and Mohammadi A.R. Experimental study of fuel regression rate in an HTPB/N_2O hybrid rocket motor. Scientia Iranica, Transactions B: Mechanical Engineering, 2018; 25(1): 253–265. https://doi.org/10.24200/sci.2017.4317